

The turbulent/non-turbulent interface and entrainment in a hypersonic boundary layer

Fanzhao Meng, Wang Han, Lijun Yang
School of Astronautics, Beihang University
Beijing, China

1 Introduction

Hypersonic aircraft and air-breathing propulsion systems are often exposed in complex flow environments where shock waves closely interact with turbulent boundary layers, which can significantly affect the performance of the aircraft and combustor. Within the shock wave/boundary layer interaction are both the high-vorticity turbulent region and the irrotational non-turbulent region. Connecting the irrotational and turbulent regions comprises two adjacent layers: a viscous superlayer and a turbulent sublayer [1]. Between these two sublayers is a turbulent/non-turbulent interface (TNTI), while the TNTI is typically used to refer to the turbulent sublayer [2].

With the help of entrainment, the kinetic energy in the non-turbulent region can enter the turbulent region to maintain the development of the turbulent boundary layer. The flow quantities are expected to change dramatically when going through the TNTI. To understand the sudden change in the TNTI, the enstrophy and kinetic energy have been analyzed in the local reference frame centered on the TNTI [3]. Furthermore, the invariants of the velocity gradient and the strain rate as well as the passive scalar on the TNTI were investigated in [4, 5]. In addition, the entrainment near the TNTI is of critical importance, which affects how the non-rotational fluid outside the turbulent interface acquires vorticity. As concluded in [1], there are two entrainment mechanisms: large-scale entrainment in local regions of TNTI with negative curvature (i.e., engulfment), and small-scale entrainment by a viscous diffusion process along the entire interface caused by irregular small-scale eddy motions (i.e., nibbling). Which mechanism is dominant has been a debate [1]. To address this, several diagnostic tools have been developed to quantify the engulfing and nibbling process. As for jets, recent findings suggest that the nibbling mechanism is dominant [6, 7]. However, previous studies have concluded that in jets and wake [8–11] the engulfment process dominates over the nibbling process. Compared to investigations of TNTI in incompressible flows, there are only a few studies about TNTI and entrainment in hypersonic boundary layers.

In this context, it is necessary to understand the entrainment mechanisms and quantitatively characterize the engulfment and nibbling processes in the hypersonic turbulent boundary layer interacting with the shock wave. To this end, a numerical simulation of hypersonic boundary layer is carried out in this work, and the TNTI is then extracted to analyze the entrainment mechanisms. This paper is organized as follows. First, the solver used in this numerical simulation and the configurations are introduced in

Section 2. The method used to extract TNTI is discussed in Section 3. The quantitative description and analysis of the entrainment mechanisms are presented in Section 4. The conclusions are given in Section 5.

2 Simulation Details

In this study, the STREAMS solver [12] is used to perform direct numerical simulation of the interaction between the hypersonic turbulent boundary layer and the shock wave. The specific conditions mimics the typical working conditions of the Purdue University Mach 6 wind tunnel experiment. The free flow Mach number $Ma = 5.86$, the inlet friction Reynolds number $Re_\tau = 375$, and the wall temperature ratio $T_w/T_r = 0.76$. The spatial discretization relies on a hybrid sixth-order central/fifth-order WENO discretization. The computational domain of $Lx \times Ly \times Lz = [70 \times 12 \times 6.5]\delta_{in}$ is discretized using the grid of $Nx \times Ny \times Nz = [2048 \times 384 \times 256]$, where δ_{in} represents the thickness of the initial boundary layer of the incoming flow. The wedge above the computational domain generates the shock wave, and the incident angle is adjusted to 8° . The interaction position between the shock wave and the boundary layer is at $60\delta_{in}$.

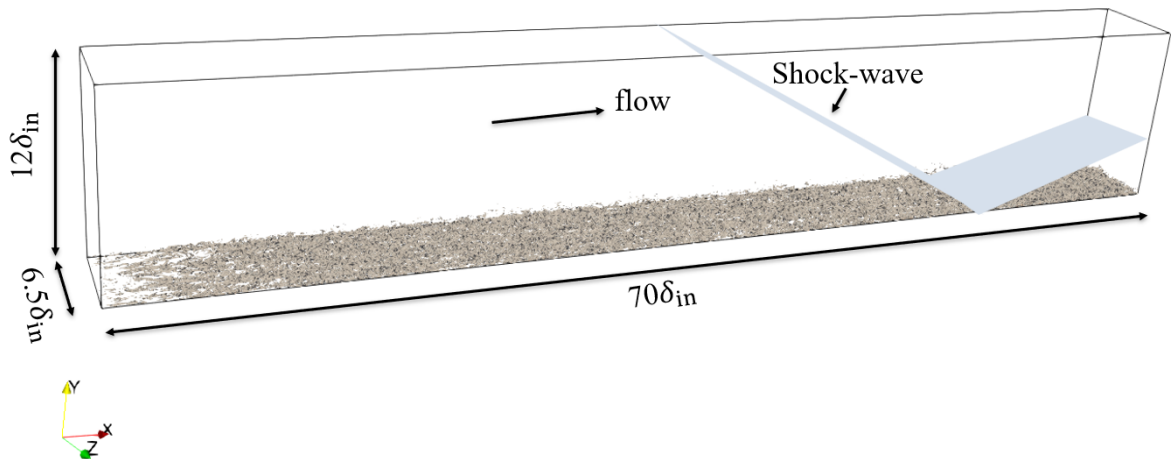


Figure 1: The hypersonic turbulent boundary layer simulated in this work, in which the gray area at the bottom represents vorticity.

3 Turbulent/Non-Turbulent Interface

Typically, thresholding methods based on vorticity [13], turbulent kinetic energy (TKE) [14], enstrophy [15] or probability density functions constructed from velocity profiles [16] are employed to extract TNTI. Among them, the method based on the vorticity threshold has been widely used [1]. However, the disadvantage of this method is that it depends on the choice of threshold value. To overcome this, the fuzzy clustering method (FCM) has been recently proposed in [6] to accurately identify the TNTI. The FCM is based on tracking the Lagrangian trajectory of fluid particles, which are bound to fluctuate violently in the turbulent region. The tracking time is limited to avoid the cumulative errors caused by the entrainment process and spanwise velocity. In the context of FCM, the TNTI is identified as the velocity fluctuation contour along the trajectory.

Figure 2 compares the results of TNTI extracted using two methods: TKE method and FCM method. The comparison shows that the novel FCM method can capture more detailed small-scale structures of

TNTI, compared to the conventional TKE method.

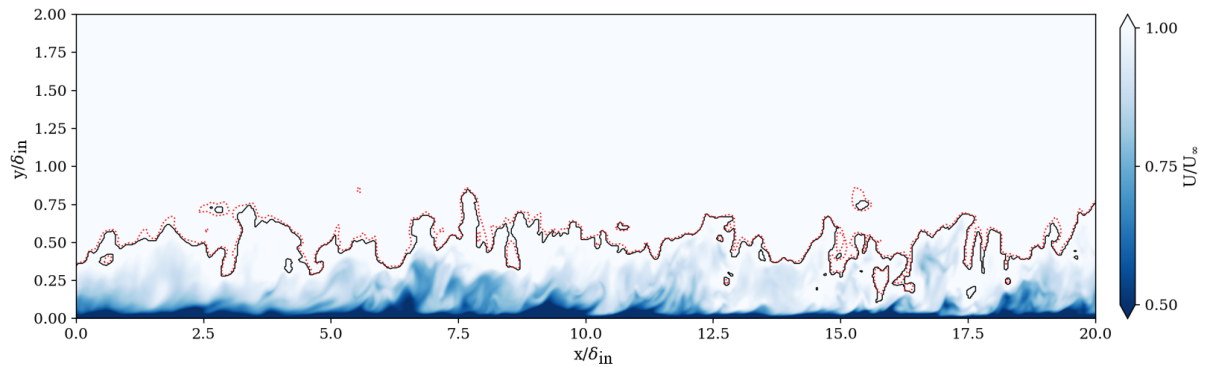


Figure 2: The turbulent/non-turbulent interfaces (TNTIs) identified by the FCM method (black solid line) and conventional TKE method (red dotted line).

4 Entrainment Mechanisms

The two entrainment mechanisms, engulfment and nibbling, will be studied in this section. The nibbling process considered a process of eddy diffusion across the TNTI is dominated by small-scale structures. The engulfment process is dominated by large-scale structures, which helps the external irrotational fluid transport into the turbulent region. To describe these two mechanisms, the velocity and mass flux are investigated in this work to distinguish the two mechanisms quantitatively.

There are three types of velocities associated with the entrainment process [1]. The first velocity is the one at which irrotational fluid crosses a boundary into the turbulent region, denoted by the induced velocity E_v . The second velocity is the diffusion velocity of the turbulent boundary to the non-turbulent flow, denoted by the boundary entrainment velocity E_b . The third velocity determines the mass flow rate through the TNTI, denoted by the local entrainment velocity V_n which is the relative velocity between the local fluid and the TNTI. In addition, previous studies concluded that the mass fluxes generated by the two mechanisms are different. Therefore, the two mechanisms in the hypersonic turbulent boundary layer will be quantitatively characterized by the velocity and mass flux in the future work.

5 Conclusion

The turbulent/non-turbulent interface (TNTI) and entrainment in a hypersonic turbulent boundary layer is investigated in this work using the direct numerical simulation (DNS) method. The conditions considered in this work mimics the Purdue University Mach 6 wind tunnel experiment. The TNTI in the hypersonic boundary layer is identified by the fuzzy clustering method (FCM). In the future, the two entrainment mechanisms (i.e., engulfment and nibbling) near the TNTI will be investigated in details.

6 Acknowledgements

This work is supported by National Natural Science Foundation of China.

References

- [1] da Silva CB, Hunt JCR, et al.(2014). Interfacial Layers Between Regions of Different Turbulence Intensity. *Annu. Rev. Fluid Mech* 46:567–90.
- [2] Worth NA, Nickels TB. (2011). Time-resolved volumetric measurement of fine-scale coherent structures in turbulence. *Phys. Rev. E* 84:025301
- [3] da Silva CB, dos Reis RJN, Pereira JCF. (2011). The intense vorticity structures near the turbulence/non-turbulent interface in a jet. *J. Fluid Mech.* 685:165–90.
- [4] da Silva CB, Pereira JCF. (2008). Invariants of the velocity-gradient, rate-of-strain, and rate-of-rotation tensors across the turbulent/nonturbulent interface in jets. *Phys. Fluids* 20:055101.
- [5] Silva TS, da Silva CB . (2017). The behaviour of the scalar gradient across the turbulent/non-turbulent interface in jets. *Phys. Fluids* 29(8).
- [6] Mathew J, Basu AJ. (2002). Some characteristics of entrainment at a cylindrical turbulent boundary. *Phys. Fluids* 14:2065–72.
- [7] Westerweel J, Fukushima C, Pedersen JM, Hunt JCR. (2005). Mechanics of the turbulent-nonturbulent interface of a jet. *Phys. Rev. Lett.* 95:174501.
- [8] Dahm WJA, Dimotakis PE. (1987). Measurements of entrainment and mixing in turbulent jets. *AIAA J.*25:1216–23.
- [9] Ferré JA, Mumford JC, Savill AM, Giralt F. (1990). Three-dimensional large-eddy motions and fine-scale activity in a plane turbulent wake. *J. Fluid Mech.* 210:371–414.
- [10] Mungal MG, Karasso PS, Lozano A. (1991). The visible structure of turbulent jet diffusion flames: large-scale organization and flame tip oscillation. *Combust. Sci. Technol.* 76:165–85.
- [11] Dimotakis PE. (2000). The mixing transition in turbulent flows. *J. Fluid Mech.* 409:69–98.
- [12] Bernardini, M, Modesti, D, et al. (2021). STREAMS: A high-fidelity accelerated solver for direct numerical simulation of compressible turbulent flows. *Computer Physics Communications*, 263, 107906.
- [13] Bisset DK, Hunt JCR, Rogers MM. (2002). The turbulent/non-turbulent interface bounding a far wake. *J. Fluid Mech.* 451:383–410.
- [14] Holzner M, Liberzon A, Nikitin N, Kinzelbach W, Tsinober A. (2007). Small-scale aspects of flows in proximity of the turbulent/nonturbulent interface. *Phys. Fluids* 19:071702.
- [15] Borrell G, Jiménez J, (2016). Properties of the turbulent/non-turbulent interface in boundary layers. *J Fluid Mech* 801.
- [16] Wu X, Wallace JM, Hickey JP, (2019). Boundary layer turbulence and freestream turbulence interface, turbulent spot and freestream turbulence interface, laminar boundary layer and freestream turbulence interface. *Phys Fluids* 31(4).
- [17] Younes K, Gibeau B, (2021). A fuzzy cluster method for turbulent/non-turbulent interface detection. *Experiments in Fluids* 62:73.